URSI GASS 2020, Rome, Italy, 29 August - 5 September 2020

Near-field measurement and far-field characterization of a high-gain Cassegrain antenna at 300 GHz band base on a photonics technology

Yusuke Tanaka(1), Hana Arisesa(1), Atsushi Kanno(2), Norihiko Sekine(2), Junichi Nakajima(3), and Shintaro Hisatake*(1)
(1) Gifu University, Gifu, Japan
(2) National Institute of Information and Communication Technology, Tokyo, Japan
(3) SoftBank, Tokyo, Japan

Abstract

Near-field antenna pattern of a Cassegrain antenna at 300 GHz was measured based on non-polarimetric electrooptic (EO) frequency down conversion technique combined with a self-heterodyne system. Measured near-field pattern of the antenna, whose diameter and designed antenna gain are 152 mm and 48 dBi, respectively, was converted to the far-field pattern to characterize the radiation pattern of the antenna. The full width at a half maximum of the antenna is obtained 0.46 deg. and 0.40 deg. for E-plane and H-plane, respectively.

1 Introduction

High gain antennas at terahertz (THz) frequency range (0.1 THz- 10 THz) have an important role in wireless communication systems for compensation of high propagation loss, which is inversely proportional to the wavelength of the radio waves. To mitigate the propagation loss, high-gain antenna should be implemented in transmitter and receiver equipment in long-range THz wireless systems. Recently, high-gain (more than 45 dBi) Cassegrain-type antennas have been developed and tested in THz wireless transmission under a transmission distance longer than 20 m [1]. In the scenario, radiation pattern is a key parameter to determine the system performance, therefore, it is necessary to accurately characterize the radiation pattern of the antennas.

The far-field pattern measurement by a vector network analyzer is commonly used in radiation pattern characterization. In principle, an antenna under test (AUT) and a probe antenna should be set under far-field condition. The distance d between the AUT and the probe is required to be at least $d=2D^2/\lambda$, so-called Fraunhofer distance, where D and λ denote the diameter of the AUT and the wavelength, respectively. For instance, a tested antenna with the diameter of D=152 mm at the frequency of 300 GHz (λ=1 mm) requires more than 46-m separation for the far-field measurement. As compared in the microwave band, the antenna pattern measurement in THz band under far-field condition is not applicable owing to the high propagation loss: resulting low signal-to-noise ratio.

In this study, we measured the near-field antenna pattern of the Cassegrain antenna in 300-GHz band using a photonics-based probe system. We also evaluated far-field pattern converted from measured near-field pattern.

2 Experimental results

Figure 1 shows a Cassegrain antenna as an AUT [2]. The diameter of the AUT is D=152 mm and the designed antenna gain is 48 dBi.

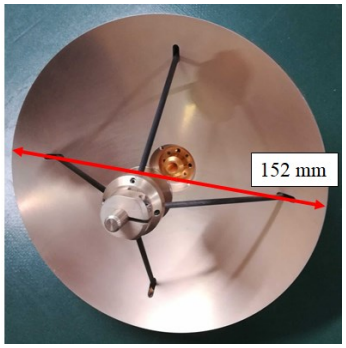

Figure 1. Cassegrain antenna.

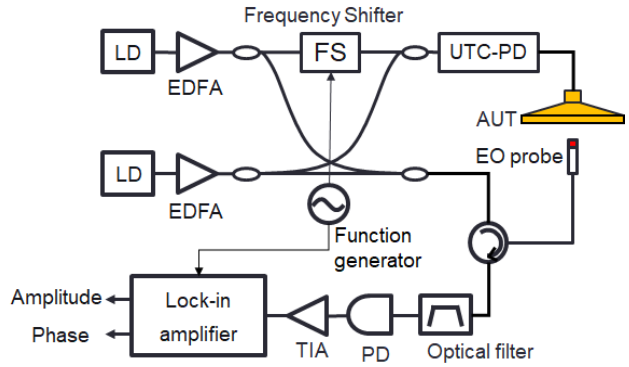

Figure 2. Near-field measurement setup. LD: laser diode, FS: frequency shifter, UTC-PD: uni-traveling-carrier photodiode, EDFA: erbium-doped optical amplifier, PD: photodiode, TIA: transimpedance amplifier.

We measured the near-field pattern based on a non-polarimetric electrooptic (EO) frequency down conversion technique [3] and self-heterodyne technique [4]. Figure 2 shows the measurement system [5, 6, 7]. The THz field is detected by an EO probe. The size of the EO crystal is 0.5

mm×0.5 mm×1 mm. The frequencies of the LDs were set to be f_1 and f_2 and combined to generate a beat note at a frequency of 300 GHz (λ=1 mm) for the RF radiation. The THz signal was generated by a uni-traveling-carrier photodiode (UTC-PD). The EO probe was set a distance of 5 mm from the antenna surface. The EO probe was moved to map the near-field (amplitude and phase) distribution. The mapped area was 160 mm×160 mm.

Figure 3 shows the measured near-field distribution. The maximum signal-to-noise ratio (SNR) of this measurement was 25 dB. The theoretically derived standard deviation of the phase measurement was 6.4 deg. Although the convex secondary reflector and support elements disturb not only the amplitude distribution but also the phase distribution, the overall phase distribution is flat. Please note, phase changes shown in right-hand side of the phase distribution might be due to the disturbance caused by our probe holder.

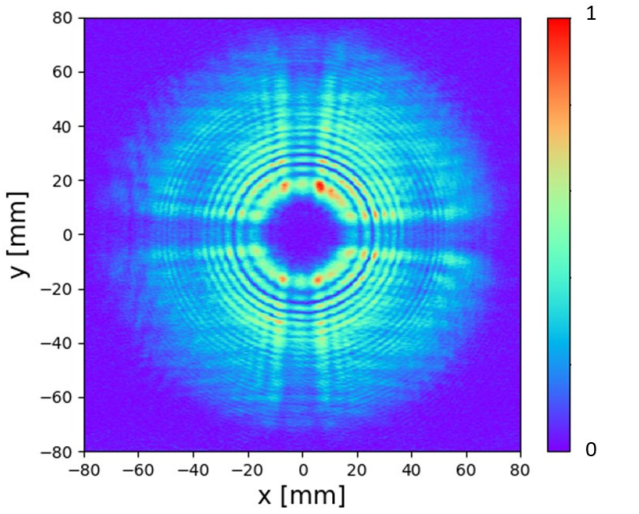

(a)

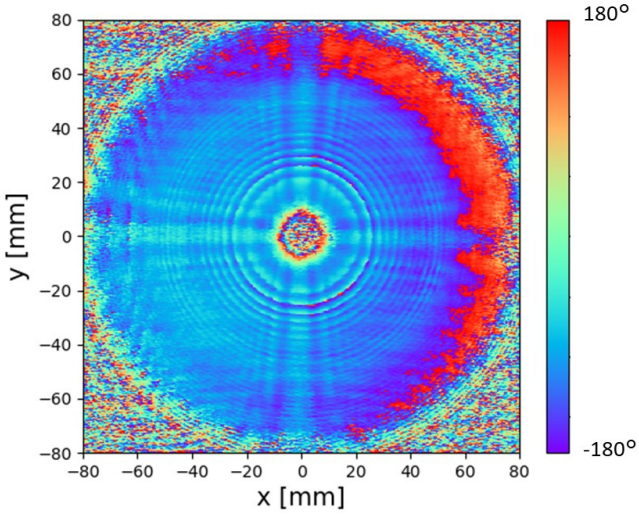

(b)

Figure 3. Measured near-field pattern. (a) Amplitude distribution, (b) Phase distribution.

The large antenna aperture size and flat phase distribution contribute to narrower beam angle. To evaluate radiation pattern of the AUT, we calculated far-field distribution form the measured near-field distribution. Figure 4 shows the calculated far-field distribution. The calculation was based on the Fourier transformation [8]. The full width at half maximum (FWHM) of the radiated beam was 0.46 deg. and 0.40 deg. for E-plane and H-plane, respectively. The small FWHM (lower divergence angle) is a key to extend the transmission distance in the THz wireless communication application.

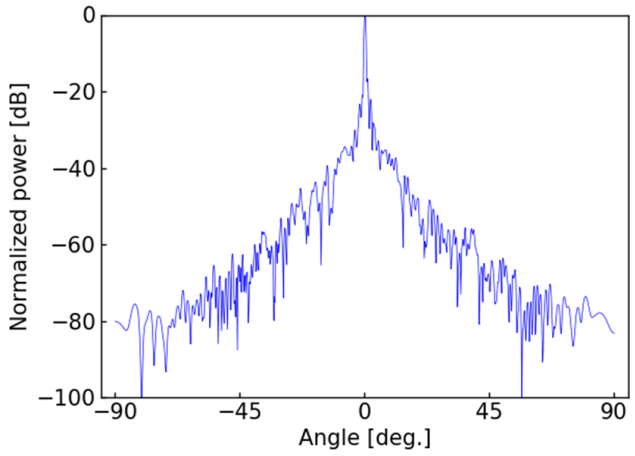

(a)

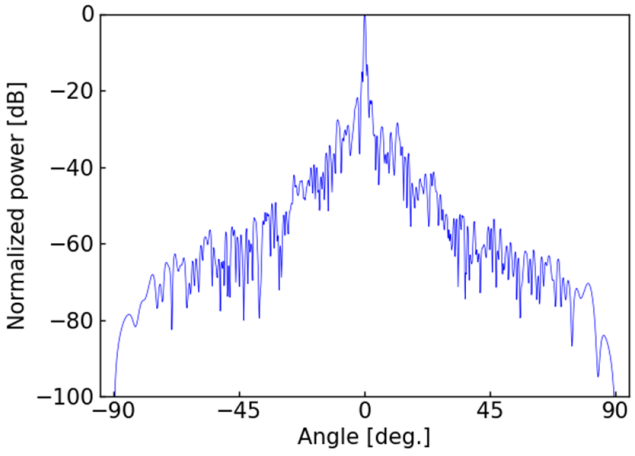

(b)

Figure 4. Calculated far-field pattern. (a) E-plane, (b) H-plane.

3 Summary

Near-field of the high-gain Cassegrain antenna was measured based on photonics technology. The radiation pattern of the Cassegrain antenna was calculated from measured near-field distribution. The antenna gain measurement will be a future work. Characterized radiation pattern based on the measured near-field pattern can be used for link budget design and interference evaluation of THz wireless communication systems.

4 Acknowledgements

This research is partially supported by funding from Horizon 2020, the European Union's Framework Program for Research and Innovation, under grant agreement No. 814523. ThoR has also received funding from the National Institute of Information and Communications Technology in Japan.

5 References

[1] C. Wang et al., "0.34-THz Wireless Link Based on High-Order Modulation for Future Wireless Local Area Network Applications," *IEEE Trans. Terahertz Sci. Technol.*, vol. 4, no. 1, pp. 75-85, Jan. 2014, Accessed on: Feb. 4, 2020. [Online]. Available doi: 10.1109/TTHZ.2013.2293119

[2] H. Sawada et al., "High gain antenna characteristics for 300 GHz band fixed wireless communication systems," in *2017 Progress in Electromagnetics Research Symposium - Fall (PIERS - FALL)*, Singapore, Singapore, Nov. 19 - 22, 2017, Accessed on: Feb. 4, 2020. [Online]. Available doi:10.1109/PIERS-FALL.2017.8293350

[3] S. Hisatake and T. Nagatsuma. "Nonpolarimetric technique for homodyne-type electrooptic field detection," *Appl. Phys. Express*, vol. 5, no. 1, Dec. 2011, Accessed on: Feb. 4, 2020. [Online]. Available doi: 10.1143/APEX.5.012701

[4] S. Hisatake, G. Kitahara, K. Ajito, Y. Fukada, N. Yoshimoto, and T. Nagatsuma, "Phase-Sensitive Terahertz Self-Heterodyne System Based on Photodiode and Low-Temperature-Grown GaAs Photoconductor at 1.55 μm," *IEEE Sens. J.*, vol. 13, no. 1, pp. 31-36, 2013, Accessed on: Feb. 4, 2020. [Online]. Available doi: 10.1109/JSEN.2012.2218281

[5] S. Hisatake, H. H. N. Pham, and T. Nagatsuma, "Visualization of the spatial–temporal evolution of continuous electromagnetic waves in the terahertz range based on photonics technology," *Optica*, vol. 1, no. 6, p. 365-371, Dec. 2014, Accessed on: Feb. 4, 2020. [Online]. Available doi: 10.1364/OPTICA.1.000365

[6] S. Hisatake, "Electrooptic field visualization and its application to millimeter-wave and terahertz antenna characterization," in *2017 IEEE Conference on Antenna Measurements & Applications (CAMA)*, Tsukuba, Japan, Dec. 4 - 6, 2017, Accessed on: Feb. 4, 2020. [Online]. Available doi: 10.1109/CAMA.2017.8273442

[7] S. Hisatake et al., "Near-field Measurement and Far-field Characterization of a J-band Antenna Based on an Electro-optic Sensing," to be presented at *EuCAP2020*, Copenhagen, Denmark, Mar. 15 - 20, 2020.

[8] Balanis, C. A., *Antenna Theory: Analysis and Design*, 2nd ed., New York: John Wiley & Sons. Inc. 1997, pp. 852-858.